Band-structure calculations for the 3d transition metal oxides in GW

Stephan Lany

Phys. Rev. B **87**, 085112 — Published 13 February 2013

DOI: 10.1103/PhysRevB.87.085112

Band-structure calculations for the 3*d* transition metal oxides in GW

Stephan Lany

National Renewable Energy Laboratory, Golden, CO 80401

Many-body GW calculations have emerged as a standard for the prediction of band-gaps, band-structures, and optical properties for main-group semiconductors and insulators, but it is not well established how predictive the GW method is in general for transition metal (TM) compounds. Surveying the series of 3d oxides within a typical GW approach using the random phase approximation reveals mixed results, including cases where the calculated band gap is either too small or too large, depending on the oxidation states of the TM (e.g., FeO/Fe_2O_3, Cu_2O/CuO). The problem appears to originate mostly from a too high average *d*-orbital energy, whereas the splitting between occupied and unoccupied *d*-symmetries seems to be reasonably accurate. It is shown that augmenting the GW self-energy by an attractive (negative) and occupation-independent on-site potential for the TM *d*-orbitals with a single parameter per TM cation can reconcile the band gaps for different oxide stoichiometries and TM oxidations states. In Cu_2O, which is considered here in more detail, standard GW based on wavefunctions from initial density or hybrid functional calculations yields an unphysical prediction with an incorrect ordering of the conduction bands, even when the magnitude of the band gap is in apparent agreement with experiment. The correct band ordering is restored either by applying the *d*-state potential or by iterating the wave functions to self-consistency, which both have the effect of lowering the Cu-*d* orbital energy. While it remains to be determined which improvements over standard GW implementations are needed to achieve an accurate ab initio description for a wide range of transition metal compounds, the application of the empirical on-site potential serves to mitigate the problems specifically related to *d*-states in GW calculations.

I. Introduction

The band-structure properties of semiconducting or insulating materials are essential for their functionality in a wide spectrum of electronic and opto-electronic applications, ranging from integrated circuits to light-emitting diodes and solar cells. Whereas conventional semiconductor technologies are mostly based on main group compounds, emerging materials often contain transition metals, examples include TiO_2 as a transparent conducting oxide [1], Fe chalcogenides [2] and Cu_2O [3, 4] as photovoltaic solar absorbers, or Fe_2O_3 as a photo-electrocatalyst [5].

Many-body perturbation theory in the GW approximation [6] has emerged as the primary computational tool for the band-structure prediction of semiconductors and insulators [7, 8, 9, 10, 11, 12, 13, 14, 15, 16, 17], providing a systematic improvement of band-structures calculated in the local density or generalized gradient approximations (LDA or GGA) to density functional theory (DFT). The past decade has seen considerable developments and discussions around a number of issues related to the GW method; concerning the technical implementation, such as pseudo-potential vs all electron methods [16, 18], the issue of core-valence partitioning [12, 16, 19] and pseudopotential scattering properties at high energies [20]; concerning convergence parameters, such as the number of unoccupied bands [21, 22]; concerning approximations for the screened Coulomb interaction W, such as the plasmon pole model [22], the random phase approximation (RPA) [14], or vertex corrections and excitonic effects beyond RPA [13, 23]; and concerning the degree of self-consistency of both the eigen-energies and the wave-functions [9, 11, 12, 13, 14, 24].

While there is presently no single universally accepted scheme for GW calculations, a fairly consistent description of band-gaps and band-structures can be achieved for *main group semiconductors and insulators*, where the following picture is emerging: (i) A single iteration of a GW update ("G_0W_0") of the single-particle energies is sufficient only if the quasi-particle energy (QPE) shifts are relatively small. Thus, one can either iterate the eigen-energies to self-consistency, or use a suitable density functional or hybrid-functional so that the initial band energies are already close to the GW QPE [14, 15, 17]. (ii) The calculation of W in the RPA leads to a significant, but systematic overestimation of the band gaps, due to an underestimated screening [11, 14]. Strategies to compensate this overestimation include a scaling of the QPE shifts [25], maintaining the screened Coulomb interaction W_0 from the first iteration for subsequent GW iterations [14], or including vertex corrections in the calculation of W interactions [13, 23, 26]. (iii) In systems with shallow 3*d* states such as the Zn-VI compounds, the 3*d* binding energy is underestimated by more than 1 eV [7, 8, 10, 13, 14]. However, the resulting effect on the band-edge states is usually rather small, except for the case of ZnO where the band gap is reduced by about 0.3 eV due to the stronger O-*p* / Zn-*d* interaction [27]. (iv) Comparing literature results from calculations with [11, 13] and without [14, 15, 17] inclusion of the non-diagonal components of the GW self-energy, it appears that the self-consistency in the wave-functions has a rather limited effect for main group compounds.

Considering *transition-metal compounds* and specifically transition-metal oxides, the situation is much less clear. While GW calculations in various flavors have been reported, e.g., for Cu_2O [24, 28, 29], TiO_2 [30] Fe_2O_3 [31] and several TM monoxides [9, 32, 33], a comprehensive study of the complete 3*d* series

of TM oxides within a single GW scheme is not available. However, surveying the present literature gives clear hints that the consistent description of TM compounds is difficult within a single approach: For example, the G_0W_0(HSE) approach (denoting a G_0W_0 calculation based on initial HSE calculation of wavefunctions and eigenvalues using the hybrid functional of Ref. [34]), that is considered to be reliable in main group compounds [15] gives a much too large band gap of 4.0 eV in Fe_2O_3 [31], compared to the experimental gap at 2.1 eV [35]. The G_0W_0(LDA) variant, which underestimates the gap of ZnO by as much as 1 eV [7, 22], already overestimates the gap by 0.3 eV in TiO_2 [30] and by 0.6 eV in $SrTiO_3$ [36]. The self-consistency in the wave-functions was found to be essential for the correct band-structure of Cu_2O [24, 28], but in ZnO and GaN, the self-consistency did not correct the underbinding of the 3*d* states [13, 37]. Thus, the purpose of the present study is to establish the trends along the 3*d* series of TM oxides in a single GW scheme.

II. Method of calculation

The GW calculations in this work are performed within the projector augmented wave (PAW) [38, 39] implementation of the VASP code [19, 39]. With the goal of a feasible scheme for high-throughput band-structure prediction in mind, computationally expedient PAW data sets were chosen for the present study: For oxygen, a "soft" potential was used, allowing for a relative small energy cutoff for the wavefunctions of 320 eV. This potential has been tested before both in density functional and GW calculations [40, 41]. For the early (Ti-Cr) and late (Mn-Cu) TM, the 3*p* shell was placed in the valence and in the core, respectively. Inclusion of the 3*s* shell in the valence for the early TM was found to lead only to marginal changes of the QPE of less than 0.1 eV. Inclusion of the 3*p* shell for the late TM had more significant effects up to few tenths of an eV, but did not lead to a systematic improvement of band gap energies compared to experiment.

The crystal and magnetic structures (NM = non magnetic, AF = anti-ferromagnetic, FI = ferri-magnetic), as well as the experimental data for band gap energies have obtained from review of the following literature: TiO_2 [42] (rutile, NM); V_2O_3 [43, 44] (monoclinic, AF); VO_2 [45] (distorted rutile, NM); V_2O_5 [46, 47] (orthorhombic, NM); Cr_2O_3 [48, 49, 50, 51] (corundum, AF); MnO [52, 53, 54] (dRS = distorted rock salt, AF); Mn_3O_4 [55, 56, 57] (hausmannite, FI); FeO [52, 58] (dRS, AF); Fe_2O_3 [35, 59, 60] (corundum, AF); CoO [52, 54, 61] (dRS, AF); Co_3O_4 [62, 63, 64] (spinel, AF); NiO [52, 65, 66, 67] (dRS, AF); Cu_2O [68, 69] (cuprite, NM); CuO [70, 71] (tenorite, AF). The crystal structures were relaxed in GGA+U [72, 73, 74] with U = 5 eV for Cu and U = 3 eV for all other 3*d* TM. These values for U have recently been found to give a consistent description of the thermochemical properties [75], and improve the description of the hybridization between the TM-*d* states with the O-*p* ligands, which is important when the wave-functions of the initial DFT calculations are maintained during the GW calculation [27]. Furthermore, the treatment of correlation effects in DFT+U is necessary in many cases to restore the correct orbital symmetries and atomic structures, since LDA or GGA are often missing Jahn-Teller like distortions in case of partially filled crystal field states of transition metal *d*-orbitals as present, e.g., in the orbital-ordered Mott insulator $KCuF_3$ [76].

For the initial GGA+U calculation of eigen-energies and wave-functions prior to the QPE calculations in GW, the cell volume was scaled so to compensate for the typical overestimation of the lattice constant

by about 1% in GGA(+U). For the Brillouin-zone sampling, a Γ-centered k-mesh was used, where the number of subdivisions was taken such to obtain at total number of at least 1000/*n* k-points, where *n* is the number of atoms in the respective unit cell. The total number of bands was taken as 64×*n*, leading to a convergence of the absolute QPE to about 0.1 eV. The energy cutoff for the response functions in GW was 150 eV. Spin-orbit interactions were not considered [77]. The HSE hybrid functional [34] has been used as an alternative Hamiltonian to generate the wavefunctions and initial eigenvalues.

III. Band gaps of 3d oxides in baseline GW calculations

As a baseline GW scheme, the screened Coulomb potential W is calculated in the random phase approximation (RPA). While the GGA+U wave-functions are fixed, the eigen-energies are iterated to self-consistency, so to remove the strong dependence of the GW result on the initial DFT band-structure energies. Before comparing the calculated band gaps with experiment, however, it is worth noting that the available experimental data for transition metal oxides is often not as comprehensive and robust as for some main group compounds (e.g., Si, GaAs, ZnO) where high-quality samples have been studied in great detail. The band gap energies of TM oxides are usually determined either by optical measurements or by photoemission / inverse photoemission. Both types of data are not free of ambiguities: In principle, the (inverse) photoemission energies correspond to the QPE calculated by GW. However, photoemission probes mostly the energies with high density of states, e.g., originating from localized TM-*d* or O-*p* states, and is less sensitive to regions with small density of states, like, e.g., the highly dispersive conduction bands occurring in many compound semiconductors. For example, the band gap of NiO, deduced from the band edge structure measured by (inverse) photoemission, has been determined as 4.3 eV [66]. Optical absorption measurements, on the other hand, show an absorption threshold at only 3.5 eV [65, 67], and the difference could be due to a smaller density of states in the conduction band that might not be resolved in the inverse photoemission measurement. The optical characterizations are, however, also subject to uncertainties if the minimum band gap is indirect or optically forbidden, or when excitonic effects, including also internal *d-d* transitions, cause strong sub-gap absorption. Thus, a given absorption onset could signify the indirect/forbidden band gap (e.g., in a bulk sample), the direct-allowed band gap (e.g., in a thin-film where phonon-assisted and disorder-induced transitions are too weak to contribute sufficiently to the absorption), the threshold for exciton generation (e.g., in wide gap systems like SiO_2 with large exciton binding energies [20]), or the excitation of internal *d-d* transitions (e.g., in Cr_2O_3 the absorption bands observed around 2.1 and 2.8 eV [49] coincide with well-known *d-d* internal excitations of octahedral Cr^{+III} [78]). These considerations need to be taken into account when interpreting optical measurements to in terms of band gap energies.

Table I: The band gap energies for the series of 3*d* oxides, comparing experimental literature data, GW in the random-phase approximation (GW^{RPA}), and GW with local-field effects and empirical V_d potentials ($GW^{LF}+V_d$). For the latter, also given are the direct (d) or indirect (i) nature of the gap, the absorption threshold energy E_{abs} for direct and allowed optical transitions [84], the electronic static electronic dielectric constant ε, and the value of the parameter V_d.

	Expt.	GW^{RPA}	$GW^{LF}+V_d$			
	E_g [eV]	E_g [eV]	E_g [eV]	E_{abs} [eV]	ε	V_d [eV]
TiO_2	3.0	4.48	3.11 (*i*)	3.4	5.9	−1.1
V_2O_3	0.6	1.70	1.07 (*i*)	1.3	6.2	−2.8
VO_2	0.6	1.12	0.46 (*i*)	0.9	9.5	
V_2O_5	2.3	4.69	1.85 (*i*)	2.4	4.9	
Cr_2O_3	3.2	4.75	3.23 (*d*)	3.3	5.9	−3.5
MnO	3.5	3.81	3.36 (*i*)	4.2	4.1	0
Mn_3O_4	2.5	2.89	2.49 (*i*)	2.5	4.7	
FeO	2.1	1.65	2.14 (*i*)	2.2	5.7	−2.0
Fe_2O_3	2.1	3.57	2.01 (*i*)	2.1	7.2	
CoO	2.8	3.23	2.80 (*i*)	3.3	5.3	−1.2
Co_3O_4	1.5	2.42	1.55 (*d*)	1.6	8.0	
NiO	3.5	4.28	3.48 (*i*)	3.7	6.5	−0.3
Cu_2O	2.2	1.59[a]	2.03 (*d*)	2.7	5.7	−2.4
CuO	1.6	2.49	1.19 (*i*)	1.4	7.9	

[a] incorrect band ordering

Table I shows the experimental band gap energies from the literature in comparison with the results of the baseline GW^{RPA} calculations, and with calculations that include an on-site potential for *d*-states as discussed in Sec. IV below. While in main group compounds, the RPA is known to lead to underestimated dielectric constants, and, hence, to overestimated band gap energies (E_g) [11, 14], it is apparent that GW^{RPA} gives mixed results with cases where the band gaps are much too large (e.g., TiO_2, V_2O_5, Cr_2O_3, Fe_2O_3) and cases where the band gaps are too small (FeO, Cu_2O). As discussed in detail in Sec. V below, in case of Cu_2O the discrepancy is much more dramatic than apparent from the band gap energy, since the band ordering is wrong in GW^{RPA}. Note that similar trends and inconsistencies are also observed when using the HSE hybrid functional instead of GGA+U to calculate the initial eigen-energies and wavefunctions. The overall agreement with experiment is obviously much worse and less systematic than for similar type of calculations in main group compounds [11, 12, 13, 14, 15, 16], suggesting that the discrepancies are associated with the presence of *d*-states close to the band edge energies.

At the present, the precise physical nature of difficulty to correctly describe the TM-*d* states in GW is not entirely clear. While the imperfect description of the dielectric constant in RPA and incomplete self-interaction correction have been discussed as possible sources of the too high energies of *occupied* 3*d* states in Zn-VI and Ga-V compounds [7, 10, 14], these effects do not readily explain the too high energies of the *unoccupied* 3*d* states that cause the too large band gaps in e.g., TiO_2, V_2O_5, and Fe_2O_3

(see Table I). It also seems presently unclear which methodological improvements are needed for an accurate ab initio GW description of transition metal compounds. While the self-consistency in the wavefunctions significantly improves the band structure in Cu_2O (Ref. [24, 28], see also below), it does not correct the *d*-band position in ZnO [13, 37]. Possible improvements may further result from excitonic effects (vertex corrections), or from improvements or more technical nature, such as the use of PAW potentials that have been specifically generated so to yield better scattering properties at very high energies [20], or the inclusion of more semi-core states being explicitly treated as valence electrons. However, all of these options will increase the computational overhead considerably.

IV. GW results with an on-site potential to adjust *d*-orbital energies

In the following, the objective is to find a workable GW scheme that allows for reasonably predictive band-structure calculation at an acceptable computational cost. As a first step to improve upon the RPA, the LDA derived local-field (LF) effects are included, which corresponds to the adiabatic-LDA approximation within time-dependent-DFT [79]. While these LF effects do not fully account for the electron-hole interaction, they lead to a somewhat increased dielectric constant ε, thereby counteracting the tendency of RPA to overestimate band gaps. Thus, in oxides the band gaps are reduced by typically 0.3 - 0.6 eV relative to the RPA, which generally improves the band gap prediction in main group oxides. For example, the direct Γ-Γ gaps of MgO, CaO, and SrO are calculated as 7.87, 7.14, and 6.03 eV in GW^{LF} with GGA wavefunctions, in good agreement with the experimental values of 7.83, 7.09, and 5.90 eV, respectively [80, 81]. (The indirect Γ-X gap of SrO is calculated at 5.45 eV, close to the experimental absorption edge at 5.30 eV [82].) In the 3*d* oxides the LF effects are, however, not sufficient to achieve acceptable agreement with experiment. For example, the gap of TiO_2 is reduced from 4.48 eV in GW^{RPA} to 4.06 eV in GW^{LF}, and the Cu_2O gap is reduced from 1.59 to 0.93 eV. Thus, while the effect in TiO_2 does not go far enough, the Cu_2O gap is now much too small.

The observation that the GW^{LF} approach is very accurate for main group compounds suggests that the band structure features due to states with *s*- and *p*- like atomic orbital character should be also accurately described in TM compounds. Then, a specific treatment of the *d*-states via an on-site potential, similar as in the DFT+U formalism [73, 74], could serve to mitigate the problems arising from the presence of *d*-states close to the band edge energies. Since the precise nature of the issues related to *d*-states in GW is yet unclear, such an approach is empirical in nature and serves as a phenomenological solution. However, a technical justification for this approach derives from the fact that the on-site potential acts exclusively on the problematic *d*-orbitals and does not affect the compatibility of the GW scheme with other *sp* elements, e.g., in ternary compounds containing both TM and main group cations. Further, if a sufficient degree of transferability of the empirical parameters is given, i.e., if the same on-site term for a given TM element improves the results systematically for multiple compounds, then this approach can be expected to provide an improved reliability for band-structure predictions in transition metal compounds within a single GW scheme.

The fact that within the present GW^{RPA} baseline approach the *d*-orbital energies lie too high in energy for both occupied *d*-shells (as in ZnO, Cu_2O) and unoccupied *d*-shells (as in TiO_2 and V_2O_5) suggests that the average *d*-orbital energy could be lowered by an attractive on-site potential for *d*-states, $V_d < 0$, to be

applied in addition to the GW self-energy operator. The common on-site potential of the DFT+U form [73] is, however, not suitable for this purpose because it creates an attractive potential $V_{\mathrm{DFT+U}} < 0$ only for occupied stated, but a repulsive potential $V_{\mathrm{DFT+U}} > 0$ for unoccupied states. Therefore, the non-local external potential of the form [83]

$$\hat{V}_{a,l} = \sum_{i,i'} |p_i\rangle\langle\phi_i|V_{a,l}|\phi_{i'}\rangle\langle p_{i'}|$$

is employed here instead, where the p and ϕ^{AE} are the PAW projectors and all electron partial waves, respectively, which depend on an index i (i') that comprises the atomic site a, the angular momentum numbers l,m and an index k for the reference energy [39]. The strength of the on-site potential is defined by the parameter V_{d} ($V_{a=\mathrm{TM},l=2}$), which in contrast to the DFT+U potential is not occupation dependent.

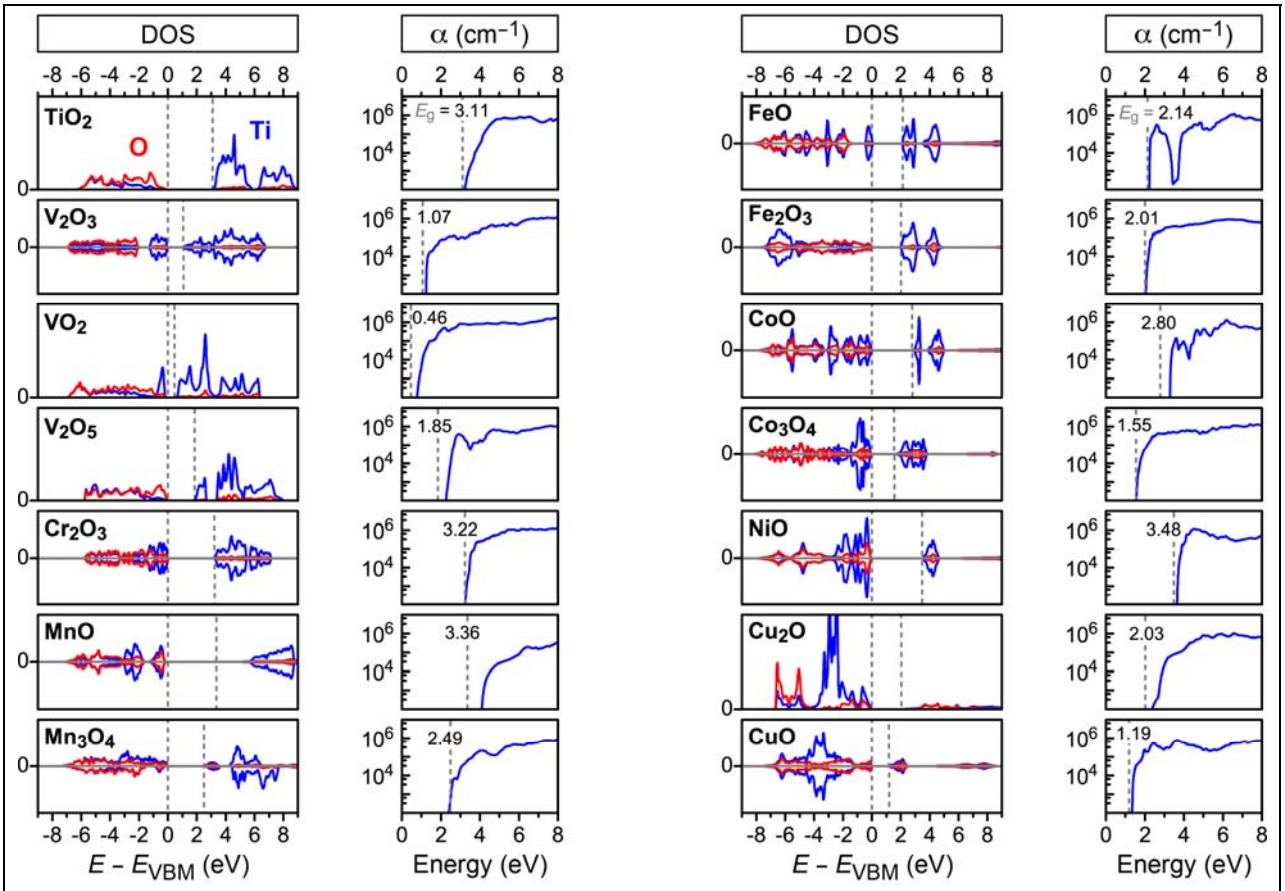

Fig. 1. The density of states (DOS) and absorption coefficient α for the 3*d* oxides calculated in $\mathrm{GW^{LF}}$+V_{d}. In spin-polarized cases, the spin-up and spin-down DOS are shown to positive and negative values. Dashed lines indicate the band gap energy E_{g}.

For each of the TM cations, the parameter V_{d} has been adjusted so to reach the best agreement with the above cited experimental data from Refs. [42-71]. The above described considerations regarding the

determination of the band gap energy from experiment have been taken into account, and, where available, the spectral dependence was considered for the adjustment (e.g., the energy dependence of the imaginary part of the dielectric function in case of V_2O_5 [47]). Table I lists the resulting band gap energy, the optical absorption threshold for direct allowed transitions [84], the electronic dielectric constant ε, and the magnitude of V_d for the respective TM cation. Figure 1 shows the local density of states and the absorption spectrum, calculated in the independent-particle approximation (i.e., excluding excitonic effects). Note that the absorption spectra also do not include phonon-assisted or disorder-induced indirect/forbidden transitions.

It is an encouraging observation that good agreement of the band gap energies with experiment can be achieved with a single parameter V_d per TM atom even in those cases where different oxide stoichiometries and TM oxidation states are available (Table I). Notably, $V_d = -2.0$ eV for Fe compensates for both the underestimated gap of FeO (E_g = 1.31 eV in GW^{LF} without V_d) and the overestimated gap of Fe_2O_3 (E_g = 3.09 eV in GW^{LF} without V_d). Similarly, also in case of the Cu-oxides, a correction of E_g in opposite directions is achieved with a single V_d parameter (Table I). Generally, one can expect that a negative value for V_d will lead to a significant increase of E_g in compounds like FeO or Cu_2O where the occupied TM-*d* states lie close to the VBM, but to a decrease of E_g in compounds like Fe_2O_3 or CuO where the unoccupied TM-*d* states lie close to the CBM (cf. Fig. 1). The observation that a single parameter V_d leads to a much improved band gap energy in either situation strongly suggests that the difficulties encountered in standard GW calculations for TM compounds relate mostly to the *average d*-orbital energy, and not so much the exchange splitting between the majority/minority spins directions or the splitting between occupied and unoccupied *d*-symmetries. Therefore, the appropriate magnitude of V_d should be rather insensitive on the local environment, and there is reason to believe that $GW^{LF}+V_d$ could be suitable for predictions of a wider range of transition metal compounds that have not yet been extensively studied experimentally. For example, we recently investigated in a related study the ternary oxide Cr_2MnO_4 [85], where the experimental band gap was determined to lie around 3.2 - 3.4 eV. While the GW^{RPA} approach largely overestimates the gap at E_g = 4.7 eV, the $GW^{LF}+V_d$ scheme yields 3.3 eV with the same parameters as determined in the present work.

V. Band ordering in Cu_2O in different GW schemes

Cu_2O is *p*-type semiconductor that recently received renewed interest as a photovoltaic and photocatalytic material [3, 4, 29, 69, 86]. While its relative large band gap of 2.17 eV is still suitable for a wide-gap solar absorber, the optical transition at the band gap energy is parity forbidden [68, 69], leading to a weak absorption onset, which is particularly detrimental in thin-film absorbers. Thus, the correct theoretical description of the energy ordering of bands with different symmetries - giving rise to allowed and forbidden transitions - is essential to realistically describe the optical properties of Cu_2O in the context of solar energy applications.

Figure 2 shows the calculated dielectric function and the absorption spectrum for Cu_2O, based on GGA+U wavefunctions and $GW^{LF}+V_d$ quasi-particle energies as described above. For the calculation of these optical spectra, excitonic effects (electron-hole interactions) are included within the time dependent hybrid functional approximation described in Ref. [79], using a constant screening factor $1/\varepsilon$

for the electron-hole exchange. Compared to previous calculations in the independent particle approximation based on a HSE band-structure [87], the spectrum of the imaginary part ε_2 shows a considerable shift of intensity to lower energies closer to the band gap, thereby improving significantly the agreement with the experimentally measured dielectric function [69, 87]. The inclusion of excitonic effects further increases the static electronic dielectric constant from ε = 5.7 (Table I) to 6.2 (experiment: ε = 6.46 [88]), and also leads to a near quantitative agreement with the experimental absorption spectrum [89, 90]. Thus, it can be concluded that the $GW^{LF}+V_d$ approach affords a very realistic description of the band-structure and optical properties of Cu_2O.

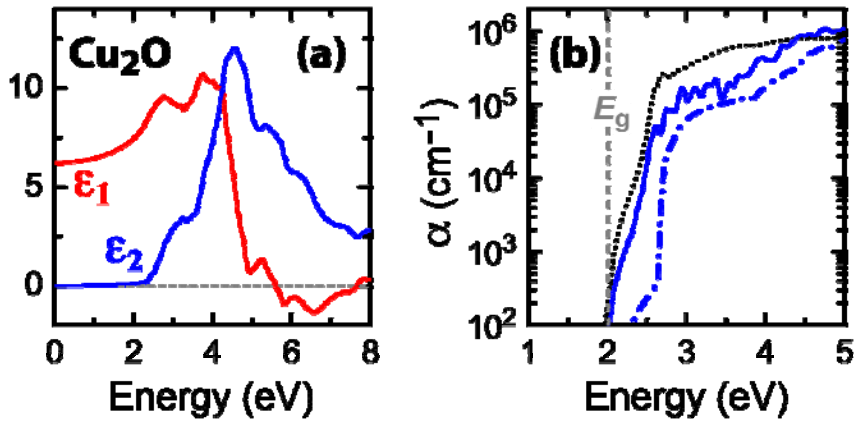

Fig. 2. (a) The real (ε_1) and imaginary (ε_2) parts of the dielectric function and (b) the absorption coefficient (α) for Cu_2O, based on the $GW^{LF}+V_d$ approach, including excitonic effects. For comparison, the experimental spectrum is shown as dotted line (after Refs. [89, 90]), and the calculated spectrum in the independent particle approximation is shown as dash-dotted line.

In order to facilitate a comparative evaluation of different GW schemes in regard of allowed and forbidden valence-to-conduction band transitions, the following discussion is intended to elucidate the origins of the peculiar conduction band structure of Cu_2O and its relation to the features of the cuprite structure.

Figure 3a shows the band-structure of Cu_2O calculated in the $GW^{LF}+V_d$ approach [91], highlighting the valence band maximum (VBM, $\Gamma_{25'}$), the conduction band minimum (CBM, Γ_1), and the second conduction band ($\Gamma_{12'}$). Figure 3b shows the cuprite structure, where the unit cell is rotated so that the O-Cu-O dumbbell motif is aligned along the *z* axis. Due to the presence of inversion symmetry in the cuprite structure with the Cu sites as inversion center (cf. central Cu site in Fig. 3b), the parity of the wavefunctions is well defined. The $\Gamma_{25'}$ VBM has dominantly a Cu-*d* atomic orbital character and is of even parity. The Γ_1 CBM has *s*-like contributions from both the cation and the anion, similar to other direct gap compounds (e.g., GaAs, ZnO, MgO). However, reflecting the symmetry of the O-Cu-O dumbbell structure (Fig. 3b), Cu-d_{z^2} and Cu-*s* orbitals share a common point group representation (a_{1g}), leading to an unusual intra-site *s*-*d* hybridization and to a strong Cu-d_{z^2} contribution to the CBM. The

parity of Γ_1 is even and, therefore, the optical transition at the band gap energy $E(\Gamma_1)$ - $E(\Gamma_{25'})$ is dipole forbidden. The second conduction band ($\Gamma_{12'}$) is doubly degenerate and has a Cu-p_{xy} character, and it can be understood as originating from the two unoccupied atomic Cu-4p_{xy} orbitals that are oriented perpendicular to the O-Cu-O dumbbell axis (cf. Fig. 3b). (The respective 4p_z-orbital oriented along the *z* axis lies at much higher energies, because it has a large overlap and hybridization with the O-*p* states of the ligands.) The $\Gamma_{12'}$ state has odd parity, hence, the vertical $\Gamma_{25'} \rightarrow \Gamma_{12'}$ transition is allowed, and causes the strong increase of absorption above about 2.5 eV [69, 90]. The energy difference $\Delta E(\Gamma_{12'} - \Gamma_1)$ = 0.45 eV between the first and second conduction bands has been experimentally determined from the four exciton series (yellow, green, blue, violet) [68, 69, 92, 93].

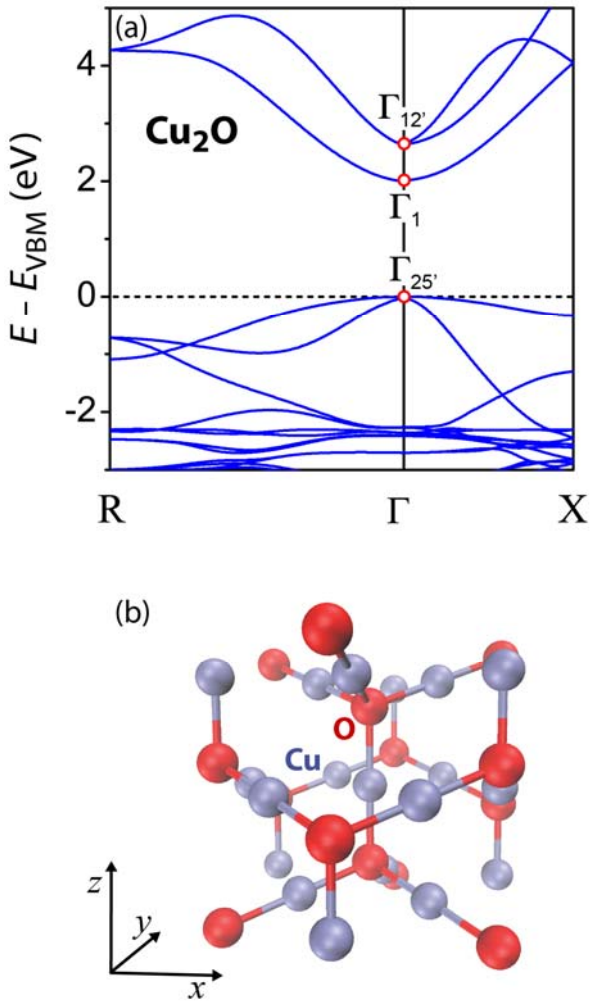

Fig. 3. (a) The band structure of Cu_2O calculated within the GW^{LF}+V_d approach, highlighting the energies of the VBM ($\Gamma_{25'}$), the CBM (Γ_1), and the second conduction band ($\Gamma_{12'}$) at the Γ point. (b) The cuprite structure, shown such to align the O-Cu-O dumbbell motif with the *z* axis.

Table II compares the band gaps E_g, the conduction band energy ordering $\Delta E(\Gamma_{12'} - \Gamma_1)$, and the static electronic dielectric constant ε in Cu_2O for a few common GW approaches besides those shown in Table I. The initial eigen-energies and wave-functions are calculated either in GGA+U as above or with the HSE hybrid functional, using the conventional parameters α = 0.25 and μ = 0.2 $Å^{-1}$ for the fraction of Fock exchange and the range-separation, respectively [34]. The GW QPE are calculated in the non self-consistent single-shot "G_0W_0", the energy self-consistent "GW", or the energy+wavefunction self-consistent "scGW" [13] schemes.

Table II: Results of different GW approaches for Cu_2O comparing the band gap energy E_g, the energy-ordering $\Delta E(\Gamma_{12'} - \Gamma_1)$ of the first two conduction band states, and the shift ΔE_{VBM} of the VBM energy relative to the initial Hamiltonian denoted in parenthesis.

	E_g (eV)	$\Delta E(\Gamma_{12'} - \Gamma_1)$	ΔE_{VBM}
Experiment	2.17	+0.45	-
GGA+U	0.72	+1.37	-
GW^{RPA}(GGA+U)	1.59	–0.28	+0.68
GW^{LF}(GGA+U)	0.93	–0.60	+1.18
GW^{LF}+V_d(GGA+U)	2.03	+0.66	–0.62
HSE	2.01	+0.51	-
$G_0W_0{}^{RPA}$(HSE)	1.91	–0.38	+0.62
GW^{RPA}(HSE)	1.54	–0.56	+1.02
$scGW^{RPA}$	2.38	+0.38	-

The following trends are observed in Table II: The GGA+U calculation underestimates E_g and overestimates the energy difference $\Delta E(\Gamma_{12'} - \Gamma_1)$ between the first and the second conduction band, reflecting the typical errors in local-density functionals. The quasi-particle energy calculation in GW^{RPA}(GGA+U) leads to a band gap that stays well below the experimental value, which is untypical for GW^{RPA} that is otherwise known for its small but systematic overestimation of band gaps due to an underestimated dielectric constant in RPA [11, 14]. Also, GW^{RPA} leads to an inversion of the conduction band ordering, now incorrectly placing Γ_1 above $\Gamma_{12'}$. The origin of these problems can be ascribed to a too high Cu-*d* orbital energy, which causes an unusual upshift of the VBM ($\Gamma_{25'}$) energy relative to GGA+U (Table II). Due to the above-described *s-d* intra-site hybridization also the Γ_1 state is strongly affected, causing the band energy inversion. (Note that the energy of the Cu-*p* like $\Gamma_{12'}$ state is remarkably invariant and stays within a narrow 0.2 eV interval for all Hamiltonians listed in Table II [94]). The inclusion of local field effects further aggravates these inaccuracies. The effect of the on-site potential V_d = -2.4 eV in the GW^{LF}+V_d approach is to lower both the $\Gamma_{25'}$ and Γ_1 states which have a strong Cu-*d* character, hence restoring the correct band ordering and band gap (cf. Table II). It should be noted that the inverted band ordering was observed before in $G_0W_0{}^{RPA}$(GGA) [28], but not in $G_0W_0{}^{RPA}$(LDA) [24, 28], indicating that the band ordering in GW can be rather sensitive on the character of the wavefunctions.

Turning towards the HSE hybrid functional as initial Hamiltonian, it is notable that the HSE calculation itself gives a good agreement for both E_g and the conduction band ordering, indicating a good description of the *d*-orbital energies (note that, in contrast, the Zn-*d* band energy in ZnO lies significantly too high in HSE [27]). In the subsequent $G_0W_0^{RPA}$(HSE) and self-consistent GW^{RPA}(HSE) calculations, the band gap is reduced and the band ordering is inverted, leading to a qualitatively wrong description similar to the GW^{RPA}(GGA+U) result. Thus, the present findings contradict the conclusion of Ref. [29], that the G_0W_0(HSE) approach appropriately describes the electronic structure of Cu_2O. As seen by the GW^{RPA} entries in Table II, the difference between the GGA+U and HSE wave-functions has only a modest effect on the final results when the eigen-energies are iterated to self-consistency.

Finally, considering the $scGW^{RPA}$ approach it is observed that the self-consistency of the wave-functions lowers the Cu-*d* orbital energy, to a similar effect as the application of the V_d potential, i.e., to lower both the $\Gamma_{25'}$ and Γ_1 states relative to the $\Gamma_{12'}$ state (cf. Fig. 3a) [94], thereby increasing the band gap and correcting the band ordering. The slight overestimation of the band gap (cf. Table II) is as expected for the RPA, indicating that the description of Cu_2O in scGW is consistent with that of main group compounds. The present result is in line with previous scGW calculations for Cu_2O [24, 28]. It is somewhat surprising that the change of the wave-functions in scGW relative to GGA+U causes changes in E_g and $\Delta E(\Gamma_{12'} - \Gamma_1)$ that are much larger and in opposite direction compared to the changes due to HSE wavefunctions (cf. Table II). This observation implies that the effect of scGW on the wavefunctions is qualitatively different from that of inclusion of Fock exchange in the HSE hybrid functional. The success of scGW for Cu_2O raises the question in how far the scGW approach can overcome in general the difficulties for transition metal compounds as described in Sec. III above. Note, however, that self-consistency of the wave-functions did not resolve the problem of the too high Zn-*d* energies in ZnO [13, 37]. Thus, a universal ab initio GW approach for TM compounds is not yet available, and may require addressing simultaneously a number of separate issues, such as vertex corrections and excitonic effects, the use of PAW potentials with improved scattering properties at high energies, or the treatment of deeper semi-core states as valence electrons, all of which increase the computational overhead. Coming at the expense of introducing one empirical parameter per TM cation, the GW^{LF}+V_d approach seems promising for reasonably accurate and computationally feasible band-structure predictions in TM compounds.

VI. Conclusions

The GW approximation has proven to be quite accurate for band-structure calculations in main group compounds, but the consistent prediction of transition metal compounds remains problematic. A range of different “flavors” of GW are currently employed in the community, differing, e.g., in the type of the Hamiltonian for the calculation of the wave-functions and initial single-particle energies, in the degree of self-consistency, and in the approximation used to calculate the screened Coulomb interaction. Thus, it is often possible to find a GW scheme that describes well a given transition metal compound, but predictions for novel materials that are not yet characterized experimentally may not be reliable. For the series of binary 3*d* transition metal oxides, a baseline GW scheme was tested here, in which the GGA+U wavefunctions are maintained, but the eigenenergies are iterated to selfconsistency, and W is calculated in the random phase approximation. This test revealed inconsistent results with cases of both

underestimation and overestimation of band gaps compared to experiment. It remains to be seen which improvements over this baseline GW scheme are ultimately needed to achieve a consistent description of electronic properties for across a wide range of transition metal compounds. In the absence of a single universal *ab initio* GW scheme that is proven to work reliably for wider range of transition metal compounds, the present work made use of the observation that the average *d*-orbital energy is the main issue, and utilized an on-site potential for the transition metal *d*-states to achieve agreement with experimental band gaps. This approach should allow for improved predictions for transition metal compounds. The photovoltaic semiconductor Cu_2O presents a particularly delicate case, where a wrong ordering of the conduction bands occurs in common GW approaches. The application of the on-site potential for Cu-*d* has been shown not only to give the correct band gap, but also to provide a consistent description of the band ordering, the dielectric function, and the absorption spectrum, which is a prerequisite for reliable predictions in the context of solar energy applications.

Acknowledgement

This work was supported by the US Department of Energy under contract No. DE-AC36-08GO28308 to NREL. The general study on band-structure prediction for the series of 3*d* oxides (results of Sec. III and IV) was supported through funds from the Office of Science, Office of Basic Energy Sciences, as part of an Energy Frontier Research Center. The more detailed study on the photovoltaic material Cu_2O (Sec. V) was supported through funds from the Office of Energy Efficiency and Renewable Energy, as part of a Next Generation Photovoltaics project within the SunShot initiative. The use of high performance computing resources of the National Energy Research Scientific Computing Center and of NREL's Computational Science Center are gratefully acknowledged.

[1] Y. Furubayashi, T. Hitosugi, Y. Yamamoto, K. Inaba, G. Kinoda, Y. Hirose, T. Shimada, and T. Hasegawa, Appl. Phys. Lett. **86**, 252101 (2005).

[2] L. Yu, S. Lany, R. Kykyneshi, V. Jieratum, R. Ravichandran, B. Pelatt, E. Altschul, H.A.S. Platt, J.F. Wager, D.A. Keszler, A. Zunger, Adv. Energy Mater. **1**, 748 (2011).

[3] A. Mittiga, E. Salza, F. Sarto, M. Tucci, and R. Vasanthi, Appl. Phys. Lett. **88**, 163502 (2006).

[4] T. Minami, Y. Nishi, T. Miyata, and J. Nomoto, Appl. Phys. Express **4**, 062301 (2011).

[5] K. Sivula, F. Le Formal, and M. Grätzel, Chem. Sus. Chem. 4, 432 (2011).

[6] L. Hedin, Phys. Rev. **139**, A796 (1965).

[7] M. Usuda, N. Hamada, T. Kotani, and M. van Schilfgaarde, Phys. Rev. B **66**, 125101 (2002).

[8] W. Luo, S. Ismail-Beigi, M.L. Cohen, and S.G. Louie, Phys. Rev. B **66**, 195215 (2002).

[9] S. V. Faleev, M. van Schilfgaarde, and T. Kotani, Phys. Rev. Lett. **93**, 126406 (2004).

[10] P. Rinke, A. Qteish, J. Neugebauer, C. Freysoldt, and M. Scheffler, New J. Phys. **7**, 126 (2005).

[11] M. van Schilfgaarde, T. Kotani, and S. Faleev, Phys. Rev. Lett. **96**, 226402 (2006)

[12] M. van Schilfgaarde, T. Kotani, and S.V. Faleev, Phys. Rev. B **74**, 245125 (2006).

[13] M. Shishkin, M. Marsman, and G. Kresse, Phys. Rev. Lett. **99**, 246403 (2007).

[14] M. Shishkin and G. Kresse, Phys. Rev. B **75**, 235102 (2007).

[15] F. Fuchs, J. Furthmüller, F. Bechstedt, M. Shishkin, and G. Kresse, Phys. Rev. B **76**, 115109 (2007).

[16] R. Gómez-Abal, X. Li, M. Scheffler, and C. Ambrosch-Draxl, Phys. Rev. Lett. **101**, 106404 (2008).

[17] A. Schleife, C. Rödl, F. Fuchs, J. Furthmüller, and F. Bechstedt, Phys. Rev. B **80**, 035112 (2009).

[18] E. Luppi, H.C. Weissker, S. Bottaro, F. Sottile, V. Veniard, L. Reining, and G. Onida, Phys. Rev. B **78**, 245124 (2008).

[19] M. Shishkin and G. Kresse, Phys. Rev. B **74**, 035101 (2006).

[20] G. Kresse, M. Marsman, L. E. Hintzsche, and E. Flage-Larsen, Phys. Rev. B **85**, 045205 (2012).

[21] B.C. Shih, Y. Xue, P. Zhang, M.L. Cohen, and S.G. Louie, Phys. Rev. Lett. **105**, 146401 (2010).

[22] M. Stankovski, G. Antonius, D. Waroquiers, A. Miglio, H. Dixit, K. Sankaran, M. Giantomassi, X. Gonze, M. Côté, and G.M. Rignanese, Phys. Rev. B **84**, 241201(R) (2011).

[23] F. Bruneval, F. Sottile, V. Olevano, R. Del Sole, and L. Reining, Phys. Rev. Lett. **94**, 186402 (2005).

[24] F. Bruneval, N. Vast, L. Reining, M. Izquierdo, F. Sirotti, and N. Barrett, Phys. Rev. Lett. **97**, 267601 (2006).

[25] A.N. Chantis, M. van Schilfgaarde, and T. Kotani, Phys. Rev. Lett. **96**, 086405 (2006).

[26] C. Franchini, A. Sanna, M. Marsman, and G. Kresse, Phys. Rev. B **81**, 085213 (2010).

[27] L. Lim, S. Lany, Y.J. Chang, E. Rotenberg, A. Zunger, M.F. Toney, Physical Review B **86**, 235113 (2012).

[28] F. Bruneval, PhD thesis, Ecole Polytechnique (2005).

[29] L.Y. Isseroff and E.A. Carter, Phys. Rev. B **85**, 235142 (2012).

[30] W. Kang and M.S. Hybertsen, Phys. Rev. B **82**, 085203 (2010).

[31] P. Liao and E.A. Carter, Phys. Chem. Chem. Phys. **13**, 15189, (2011).

[32] C. Rödl, F. Fuchs, J. Furthmüller, and F. Bechstedt, Phys. Rev. B **79**, 235114 (2009).

[33] H. Jiang, R.I. Gomez-Abal, P. Rinke, and M. Scheffler, Phys. Rev. B **82**, 045108 (2010).

[34] A. V. Krukau, O. A. Vydrov, A. F. Izmaylov, and G. E. Scuseria, J. Chem. Phys. **125**, 224106 (2006).

[35] I. Balberg and H.L. Pinch, J. Mag. Magn. Mater. **7**, 12 (1978).

[36] R.F. Berger, C.J. Fennie, and J.B. Neaton, Phys. Rev. Lett. **107**, 146804 (2011).

[37] A.R.H. Preston, A. DeMasi, L.F.J. Piper, K.E. Smith, W.R.L. Lambrecht, A. Boonchun, T. Cheiwchanchamnangij, J. Arnemann, M. van Schilfgaarde, and B.J. Ruck, Phys. Rev. B **83**, 205106 (2011).

[38] P. E. Blöchl, Phys. Rev. B 50, 17953 (1994).

[39] G. Kresse and D. Joubert, Phys. Rev. B **59**, 1758 (1999).

[40] S. Lany and A. Zunger, Phys. Rev. B **78**, 235104 (2008).

[41] S. Lany and A. Zunger, Phys. Rev. B **81**, 113201 (2010).

[42] J. Pascual, J. Camassel, and H. Mathieu, Phys. Rev. B **18**, 5606 (1978).

[43] S. W. Lovesey, K. S. Knight, and D. S. Sivia, Phys. Rev. B **65**, 224402 (2002).

[44] V. Simic-Milosevic, N. Nilius, H.P. Rust, and H.J. Freund, Phys. Rev. B **77**, 125112 (2008).

[45] V. Eyert, Ann. Phys. **11**, 650 (2002), and references therein.

[46] V. Eyert, K.H. Höck, Phys. Rev. B **57**, 12727 (1998), and references therein.

[47] V. G. Mokerov, V. L. Makarov, V. B. Tulvinskii, and A. R. Begishev, Opt. Spectrosc. **40**, 58 (1976).

[48] T.R. McGuire, E.J. Scott, and F.F. Grannis, Phys. Rev. **98**, 1562 (1955).

[49] C.S. Cheng, H. Gomi, and H. Sakata, Phys. Stat. Sol. (a) **155**, 417 (1996).

[50] T. Ivanova, M. Surtchev, and K. Gesheva, Phys. Stat. Sol. (a) **184**, 507 (2001).

[51] S.A. Chambers, J.R. Williams, M.A. Henderson, A.G. Joly, M.Varela, and S.J. Pennycook, Surf. Sci. **587**, L197 (2005).

[52] W.L. Roth, Rhys. Rev. **110**, 1333 (1958).

[53] T. Usani and T. Masumi, Physica **86-88** B+C, 985 (1977).

[54] H.H. Chou and H.Y. Fan, Phys. Rev. B **10**, 901 (1974).

[55] G.B. Jensen and O.V. Nielsen, J. Phys. C: Solid State Phys. **7**, 409 (1974)

[56] D.P. Dubal, D.S. Dhawale, R.R. Salunkhe, S.M. Pawar, V.J. Fulari, C.D. Lokhande, J. Alloys Comp. **484**, 218 (2009).

[57] H.Y. Xu, S.L. Xu, X.D. Li, H. Wang, and H. Yan, Appl. Surf. Sci. **252**, 4091 (2006)

[58] H.K. Bowen, D. Adler, and B.H. Auker, J. Solid State Chem. **12**, 355 (1975).

[59] L. Neel, Ann. phys. 3, 137 (19478); 4, 249 (1949).

[60] C.G. Shull, W.A. Strauser, and E. O. Wollan, Phys. Rev. **83**, 333 (1951).

[61] G.W. Pratt jr. and R. Coelho, Phys. Rev. **116**, 281 (1959).

[62] W.L. Roth, J. Phys. Chem. Solids **25**, 1 (1964).

[63] K.J. Kim and Y.R. Park, Solid State Comm. **127**, 25 (2003).

[64] P.S. Patil and C.D. Lokhande, Thin Solid Films **272**, 29 (1996).

[65] R. Newman and R.M. Chrenko, Phys. Rev. **114**, 1507 (1959).

[66] G.A. Sawatzky and J. W. Allen, Phys. Rev. Lett. **53**, 2339 (1984).

[67] Z. Zhang, Y. Zhao, and M. Zhu, Appl. Phys. Lett. **88**, 033101 (2006).

[68] S. Nikitine, *Excitons*: *Optical Properties of Solids* (Plenum Press, 1969).

[69] B.K. Meyer, A. Polity, D. Reppin, M. Becker, P. Hering, P. J. Klar, Th. Sander, C. Reindl, J. Benz, M. Eickhoff, C. Heiliger, M. Heinemann, J. Blasing, A. Krost, S. Shokovets, C. Müller, and C. Ronning, Phys. Stat. Sol. (b) **249**, 1487 (2012), and references therein.

[70] B.V. Karpenko, A.V. Kuznetsov, and V.V. Dyakin, J. Phys.: Cond. Mat. 8, 1785 (1996).

[71] F. Marabelli, G.B. Parravicini and F. Salghetti-Drioli, Phys. Rev. B **52**, 1433 (1995).

[72] J.P. Perdew, K. Burke, and M. Ernzerhof, Phys. Rev. Lett. **77**, 3865 (1996).

[73] V.I. Anisimov, J. Zaanen, and O.K. Andersen, Phys. Rev. B **44**, 943 (1991).

[74] S.L. Dudarev, G. A. Botton, S. Y. Savrasov, C. J. Humphreys, and A. P. Sutton, Phy. Rev. B **57**, 1505 (1998).

[75] V. Stevanovi´c, S. Lany, X. Zhang, and A. Zunger, Phys. Rev. B **85**, 115104 (2012).

[76] A.I. Liechtenstein, V.I. Anisimov, and J. Zaanen, Phys. Rev. B **52**, R5467 (1995).

[77] Non-collinear spin configurations, such as in Mn_3O_4 (see Ref. [55]) were approximated by the closest corresponding collinear configuration.

[78] B.M. Weckhuysen and R.A. Schoonheydt, Zeolites **14**, 360 (1994).

[79] Paier, M. Martijn, and G. Kresse, Phys. Rev. B **78**, 121201(R) (2008).

[80] R.C. Whited, C.J. Flaten, W.C. Walker, Solid State Commun. 13, 1903 (1973).

[81] A.S. Rao, R.J. Kearney, Phys. Status Solidi (b) **95**, 243 (1979).

[82] B. Ulrici, W. Ulrici, N.N. Kovalev, Sov. Phys. Solid State 17 2305 (1976).

[83] S. Lany, H. Raebiger, and A. Zunger, Phys. Rev. B **77**, 241201(R) (2008).

[84] The optical absorption threshold in Table I is determined from the calculated spectrum (cf. Fig. 1) somewhat arbitrarily at $\alpha = 10^3$ cm^{-1}.

[85] H. Peng, A. Zakutayev, S. Lany, T.R. Paudel, M. d'Avezac, A. Zunger, J.D. Perkins, D.S. Ginley, A.R. Nagaraja, N.H. Perry, T.O. Mason (unpublished).

[86] A. Paracchino, V. Laporte, K. Sivula, M. Grätzel, and E. Thimsen, Nat. Mater. **10**, 456 (2011).

[87] J.W. Park, H. Jang, S. Kim, S.H. Choi, H. Lee, J. Kang, and S.H. Wei, J. Appl. Phys. **110**, 103503 (2011).

[88] M. O'Keeffe, J. Chem. Phys. **39**, 1789 (1963).

[89] T. Ito, T. Kawashima, H. Yamaguchi, T. Masumi, and S. Adachi, J. Phys. Soc. Jpn. 67, 2125 (1998).

[90] C. Malerba, F. Biccari, C.L.A. Ricardo, M. d'Incau, P. Scardi, A. Mittiga, Solar Energy Mater. Solar Cells **95**, 2848 (2011).

[91] To calculate the band-structure and optical properties (Figs. 2 and 3), a finer k-mesh of 16×16×16 was used for the 6 atom primitive cell of Cu_2O. In order to keep the computational load feasible, the response functions were calculated with a reduced energy cutoff (120 eV) and k-mesh (4×4×4), and the number of bands was reduced to 256. Sub-gap features in the absorption spectrum, stemming from broadening due to the complex shift used in the Kramers-Kronig transformation, have been subtracted.

[92] J.B. Grun, M. Sieskind, and S. Nikitine, J. Phys. Chem. Solids **19**, 189 (1961).

[93] A. Dunois, J.L. Deiss, and B. Meyer, J. Phys. (Paris) **27**, 142 (1966).

[94] In plane-wave methods, the band energies are defined modulo a constant and are conventionally calculated with respect to the average electrostatic potential. If the wave-functions, and hence, the charge density are kept constant, this reference is maintained and the eigen-energies obtained for a given Hamiltonian (e.g., GW) can be expressed as a shift relative to the respective energies in the initial Hamiltonian. For the present calculations, the invariance of the energy of the $\Gamma_{12'}$ state within a 0.2 eV interval suggests that a possible "drift" of the potential reference due to differences of the wave-functions between GGA+U, HSE and scGW is small.